CHEMICAL ENGINEERING TRANSACTIONS
VOL. 97, 2022
A publication of AIDIC
The Italian Association of Chemical Engineering
Online at www.cetjournal.it
Guest Editors: Jeng Shiun Lim, Nor Alafiza Yunus, Jiří Jaromír Klemeš

ISBN 978-88-95608-96-9; **ISSN** 2283-9216
DOI: 10.3303/CET2297015

Fabrication of Chitosan-Based Film by Incorporating with Nanocellulose Produced from Agricultural Waste

Chi Thi Xuan Nguyen[a,b], Khue Hai Bui[a,b], Nhi Vo[a,b], Tan M. Le[a,b], Co Dang Pham[a,b], Nga Hoang Nguyen Do[a,b], Phong Thanh Mai[a,b], Anh Kien Le[c], Phung Thi Kim Le[a,b,*]

[a]Refinery and Petrochemical Technology Research Centre, Ho Chi Minh City University of Technology (HCMUT), 268 Ly Thuong Kiet Street, District 10, Ho Chi Minh City, Vietnam
[b]Vietnam National University Ho Chi Minh City, Linh Trung Ward, Thu Duc District, Ho Chi Minh City, Vietnam
[c]Institute for Tropical Technology and Environmental Protection, 57A Truong Quoc Dung Street, Phu Nhuan District, Ho Chi Minh City, Vietnam
phungle@hcmut.edu.vn

Oil-based plastics, a popular material in the packaging industry with inexpensive and long-lasting durability, have become a significant threat to the ecosystem due to their single-use, recalcitrant nature. Therefore, finding biodegradable plastic to replace oil-based plastics has attracted more interest. Nanocellulose and chitosan, an abundant polymer in nature, have remarkable properties such as biodegradability, bioavailability, and biocompatibility. Both materials can be produced from low-cost sources such as lignocellulosic biomass and crustacean waste, respectively. Hence, in this study, nanocellulose from agro-waste and chitosan from shrimp waste were combined to create a biofilm food packaging. The biofilms were characterized using FTIR, TGA, SEM, while the physical properties of the biofilm demonstrated the role of nanocellulose in biofilm reinforcement. As a result, PVA/CS/CNC film exhibited tensile strength up to 18.25 MPa and water resistance up to 160 % compared to the control sample. This biodegradable film offers a potential alternative to synthetic materials like food packaging.

1. Introduction

The constantly growing production and use of petroleum-based plastic has created a large amount of long-lasting material which leads to a huge accumulation of plastic waste, gradually destroying the environment and ecosystem (Selvamurugan and Pramasivam, 2019). Therefore, as cheap and convenient as oil-based plastic can be, the demand for a more environmental-friendly and biodegradable material is rising. Recently, there have been studies on plastic derived from plants or animal products, called bioplastic. This approach not only can reduce the CO_2 emitted during the plastic production, using, and recycling, but is also more economical as it substitutes petroleum with materials from agriculture (Ibrahim et al., 2021). However, unlike their synthetic counterparts, bioplastics are more vulnerable to water and exhibit lower mechanical strength (Xia et al., 2021). Thus, developing bioplastics with balanced degradability and durability is still attracting much attention.
Among the agents to improve bioplastic durability, nanocellulose (NC) is increasingly investigated due to its non-toxicity, biocompatibility, biodegradability, and high tensile strength. Moreover, NC is derived from renewable and available sources, which makes it a potential candidate in bioplastic reinforcement. In fact, the addition of NC in the composite material has been proved to improve physical, thermal, and barrier properties (Amara et al., 2021). NC can bind to other components through van der Waals forces, covalent bonds, molecular entanglement, and mechanical interlocking with the polymer matrix in the composite (Trache et al., 2020). On the other hand, the abundant hydroxyl group in the NC surface easily interacts with other substances to modify them (Reshmy et al., 2020).Previous studies showed that CNC incorporation is more effective than CNF in improving the mechanical properties of biocomposites, such as Young's modulus, tensile strength, strain-at-failure, and fracture toughness (Zhang et al., 2019).

Paper Received: 31 May 2022; Revised: 24 July 2022; Accepted: 28 July 2022
Please cite this article as: Nguyen C.T.X., Bui K.H., Vo N., Le T.M., Pham C.D., Do N.H.N., Mai P.T., Le A.K., Le P.T.K., 2022, Fabrication of Chitosan-Based Film by Incorporating with Nanocellulose Produced from Agricultural Waste, Chemical Engineering Transactions, 97, 85-90 DOI:10.3303/CET2297015

Agricultural wastes such as fruit leaves, cereal straws, or husks have a high cellulose content. However, most agro-wastes are either burned, which pollutes the air, or used as fertilizer instead of being used in a more economically valuable way (Nguyen et al., 2021). Pineapple is the second-largest harvested fruit, according to the Food and Agriculture Organization (Shahbandeh., 2021), and pineapple leaves (PLs) are also rich in cellulose with a cellulose content of about 36.3 % (Santos et al., 2013). Therefore, besides applications in spinning textiles, fertilizers for agriculture, reinforcing fillers for building materials (Asim et al., 2015). PLs are valuable as a source to produce NC.

The production of NC from agro-waste such as PLs is a potential approach to add value to agricultural residues. Therefore, the aim of this study was to isolate CNC from this abundant natural source for the reinforcement of biocomposite films. The cellulose from PLs was recovered using two-step alkalization and bleaching with hydrogen peroxide. CNC was produced using a one-step acid hydrolysis, which was then employed in high-speed homogenization to further reduce the crystal size. Moreover, the addition of PEG was effective in increasing the stability of the suspension. The rigid CNC was used to reinforce PVA/CS film, presenting a facile and cost-effective route to improve the properties of bioplastics with inexpensive PLs.

2. Materials and experimental

2.1 Materials

PLs were gathered, cleaned, dried, and ground to 80 meshes in a blender. The chemicals in this study, including sodium hydroxide (NaOH, ≥ 96.0 %), hydrogen peroxide (H_2O_2, ≥ 30.0 %), sulfuric acid (H_2SO_4, ≥ 98.0 %), acetic acid (CH_3COOH, ≥ 99.5 %), and polyvinyl alcohol (PVA), were purchased from Xilong; poly ethylene glycol (4000 PEG) from Taiwan, and chitosan solid (≥ 75.0 % deacetylated, viscosity 150 – 500 cP) from Vietnam.

2.2 Preparation of CNC from PL

PLs powder was treated 3 times with 3 % NaOH solution at a ratio of 1:20 (g/mL) for 2 h at 80 °C. The obtained solid was washed several times with distilled water until reaching neutral pH. After the alkali treatment, the material was bleached at a 1:20 (g/mL) ratio using a mixture of 10 % H_2O_2 and 1 % NaOH solution at 80 °C for 1 h. Subsequently, the solid was washed with distilled water until the pH became neutral and then dried at 80 °C. Cellulose-rich pulp after the pretreatment process was hydrolyzed with 64 % H_2SO_4 at a ratio of 1:20 (g/mL) at 45 °C for 1 h. The reaction was stopped by adding RO water to the mixture. The sample was centrifuged to remove acid and exchanged pH by using a dialysis membrane until the sample reach neutral pH to obtain CNC.

2.3 Synthesis of PVA/CS/CNC biocomposite films

The CNC suspension was homogenized for 30 min with the addition of PEG at 2 wt% to assist dispersion. PVA (3 g) was dispersed in 100 mL of H_2O for 1 h at 80 °C. Simultaneously, 1.5 g of chitosan was dispersed in 100 mL of 1 wt% CH_3COOH at 50 °C for 30 minutes until completely dissolved. The two solutions were then combined and ultrasonicated for 15 min. CNC-PEG suspension (2 g, 1 wt% CNC) was added to the solution and ultrasonicated for another 15 min. Finally, the mixture was cast onto a mold and dried at 70 °C for 2 days.

2.4 Characterizations

X-ray diffraction (XRD) patterns were collected on a Bruker D8 Advance with CuKα radiation (λ = 0.154 nm), operating voltage of 40 kV, current of 40 mA, and 2θ=10-30°. The crystallinity Index (CrI) was calculated according to a previous study (Plermjai et al., 2018). Fourier transform infrared (FTIR) spectra was obtained using a Bruker Tensor 37 spectrometer with wavenumbers in the range of of 500-4,000 cm^{-1}. Thermogravimetric analysis (TGA) was performed on a LINSEIS DSC PT 1600 in air atmosphere at a heating rate of 5 °C/min from room temperature to 1000 °C. The surface morphology of the samples was examined using a Prisma E scanning electron microscope (SEM) with a 10 kV operation voltage. Transmission electron microscopy (TEM) was performed on a JEM-1400 at 100 keV at room temperature. Apparent size distribution and zeta potential of NC sample (0.5 wt%) was studied using a Malvern Zetasizer Nano ZS90.

The tensile strength of the film sample (150 x 2.5 mm) was measured at room temperature using a ZwickRoell Z010 tensile strength meter with the pulling speed is 1 mm/min, according to DIN EN ISO 527 standards. Swelling test was performed on a 30x30 mm film sample. The sample was dried and then immersed in water at 25 °C for 2 min, 10 min, 30 min, 120 min. At each time, the sample was taken out of the water and the free water on its surface was eliminated. The swelling percentage was calculated following Eq(1).

$$\text{Swelling percentage}\,(\%) = \left[\frac{W_s - W_i}{W_i}\right] \times 100 \quad (1)$$

3. Results and discussion

3.1 CNC from PL-derived pulp

Cellulose-rich pulp (CE) was obtained after pretreatment steps including alkaline treatment and bleaching with 91.66 % cellulose content and was much higher than previous study when bleaching with NaOH/NaClO mixture (85.5 %) (Ismail et al., 2018). In addition, chlorinated chemicals such as $NaClO_2$ and NaClO used in the bleaching treatment process produce chlorolignins, which is harmful to the environment (Mussatto et al., 2008). NC was produced using chemical method which involved one-step acid hydrolysis in 1 h and homogenization. This combination played a role in reducing chemical waste compared to some previous studies employing multiple-step treatments over prolonged duration or requiring the use of high-pressure apparatuses (Balakrishnan et al., 2017; Mahardika et al., 2018). The acid hydrolysis step successfully removed the amorphous region of cellulose, as XRD patterns in Figure 1a shows that the calculated crystallinity index (CrI) of the NC sample after acid hydrolysis (CNC) increased from 68.31 % in CE to 84.21 %. This was also higher than in previous studies, in which the CrI of NC from PLs ranged from 69.52 % (Cherian et al., 2010) was synthesized by mechanical method to 73.62 % (Santos et al., 2013) was synthesized with the same hydrolysis acid method. The decomposition temperature of NC sample was also reduced after hydrolysis (Figure 1b). This decrease in thermal stability might be due to the incorporation of sulfate groups on the surface which increases thermal degradation (Nair et al., 2014). Currently, the main applications of CNC are as reinforcement for thermoplastic materials (Cheng et al., 2015), so the thermal stability of CNC is a key factor for the application of CNC as a nanocomposite material.

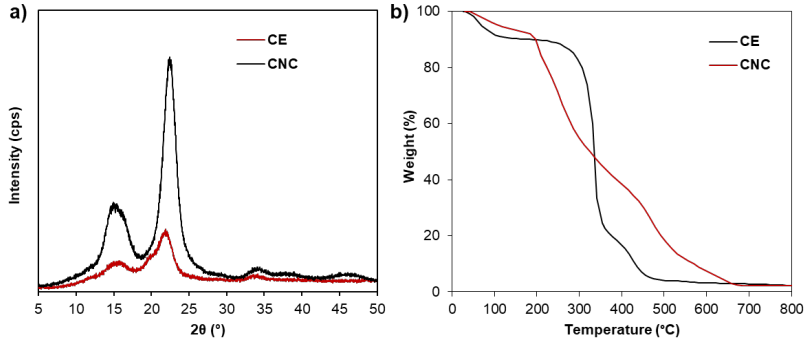

Figure 1: (a) XRD patterns and (b) TGA graph of cellulose (CE) and acid hydrolyzed NC (CNC)

The morphology and size of NC from PL was evaluated by TEM and DLS techniques. From the TEM images (Figure 2a), the NC was observed to be rod-like crystals (CNC), 10-50 nm in diameter and 75-150 nm in length. The homogenized samples (CNC-H) clearly exhibited smaller and longer shape, with diameter of 10-15 nm and around 100 nm in length. The decrease of crystal size was also confirmed by the particle size distribution using DLS (Figure 2b).

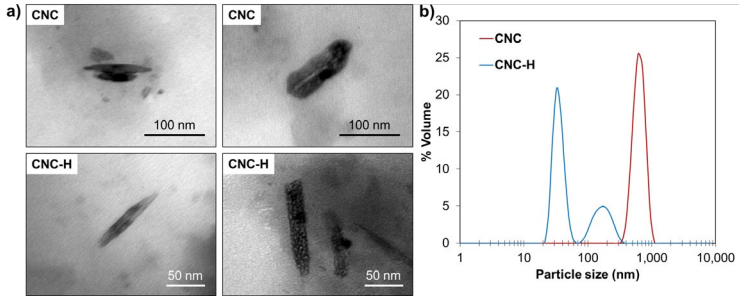

Figure 2: (a) TEM images and (b) particle size distribution graph of samples before and after homogenization.

The suspension stability of the samples was also evaluated through zeta potential. As can be seen from Table 1, the zeta potential of hydrolyzed and homogenized samples were -14.8 and -17.4 mV, respectively. In general, homogenization helps the particles distribute more evenly. However, excessive use of homogenizing may lead to destruction of the CNC particles (C.S et al., 2016), reducing the surface charge of the particles. This was evident by the zeta potential increasing from -20.4 to -17.2 mV, which means the sample was more prone to deposition. Hence, to aid dispersibility, PEG was added (CNC-PEG), increasing the zeta potential to -27.3 mV.

PEG forms hydrogen bonds with the hydroxyl groups of cellulose, leading to a decrease in surface charge in the solution. In addition, as shown in Figure 3a, when a PEG chain adheres to the surface of CNC beads, it encounters another similar chain that will generate steric repulsion, which helps the particles separate and create system stability. The wrapping of PEG chains around CNC also explained for the increase in size compared to the unmodified sample (El Miri et al., 2015).

Table 1: Average particle size by DLS and zeta potential of NC samples

	CNC	CNC-H	CNC-PEG
Average particle size (nm)	707.05 ± 8.52	157.44 ± 0.44	476.05 ± 22.12
Average zeta potential (mV)	-14.8 ± 0.7	-17.4 ± 0.2	-27.3 ± 0.2

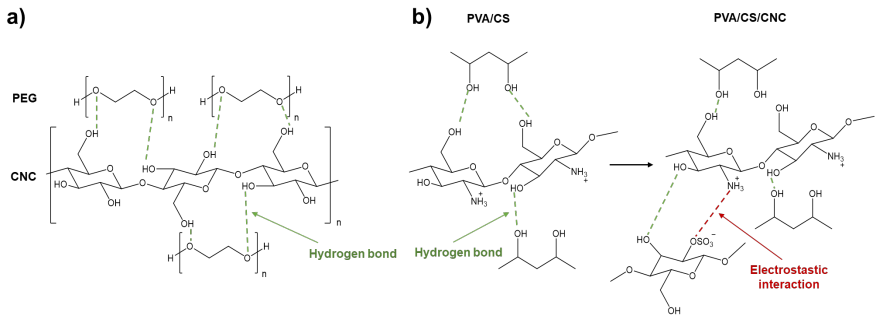

Figure 3: (a) Chemical structure of the CNC-PEG chain and (b) interactions among cellulose, chitosan and PVA

3.2 Bio-film reinforced by CNC

CNC-PEG was incorporated into PVA/CS film to enhance its properties. The morphology of the PVA/CS and PVA/CS/CNC film was analyzed by SEM technique (Figure 4). It can be observed that in Figure 4a, the surface of PVA/CS is even but has small grooves, which hinders the mechanical properties of the material. After adding CNC (Figure 4b), the gaps are filled and the surface of the film is rougher due to the uneven distribution of CNC particles. There is an improvement in adhesion and interfacial bonding between the polymer matrix and CNC due to the incorporation of surface modified CNC in the composite system, which was mentioned in a previous study by Shojaeiarani et al in 2021 (Shojaeiarani et al., 2021). In addition, the strong interaction between hydroxyl groups on the surface of CNC may also be responsible for the slight agglomeration in the film matrix.

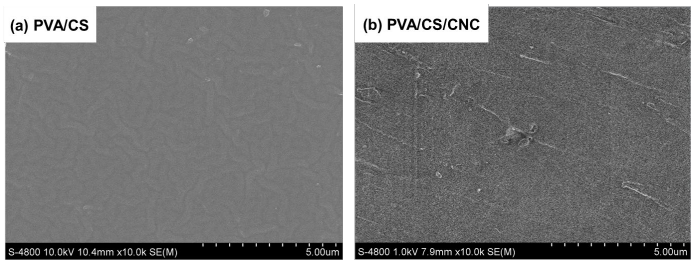

Figure 4: SEM image of samples (a) PVA/CS and (b) PVA/CS/CNC.

FTIR spectra of both film samples (Figure 5a) reveals a broad band at 3,000-3,600 cm^{-1}, which is characteristic of -OH groups in PVA, chitosan, and cellulose, and of the NH linkage in chitosan (El Achaby et al., 2017). The bands at 2,936 cm^{-1} and 1,570 cm^{-1} are the evidence of $–CH_2$ stretching vibrations and N-H bending of the primary amine in chitosan, respectively. The spectrum of PVA/CS/CNC film also exhibits a peak at 1,255 cm^{-1}, which corresponds to the asymmetric oscillation of the S=O bond in $-SO_3^-$ group on the surface of the H_2SO_4-hydrolyzed NC. The peak 1,732 cm^{-1} signals the presence of a C=O formed by the condensation of –OH and –COOH in acetic acid to give a carbonyl ester (C=O) (Khalid et al., 2021). The thermal stability of membranes was investigated by TGA (Figure 5b). The first drop in mass from 50-100 °C is related to the evaporation of water absorbed inside the material. It is also noticeable that the amount of moisture in the film with CNC incorporated was also slightly lower than the original PVA/CS. This could be due to the NC dispersion creating an interwoven network system and preventing water absorption of the film when exposed to moisture. The initial

decomposition temperature of PVA/CS and PVA/CS/NC films were 248 °C and 274 °C, respectively. Although CNC is a thermally unstable nanomaterial with the decomposition process starts at about 223 °C due to the presence of sulfate groups on the surface of the particles, when incorporated to PVA/CS film it creates a complex biological network (Figure 3b) and improves thermal stability of the PVA/CS chain (Wang et al., 2018).
The tensile strength of PVA/CS film increased from 11.40 ± 1.00 to 18.25 ± 2.05 MPa with the addition of CNC, which is 2.5 times higher than previous study synthesizing nanocomposites from oil palm empty fruit bunch fiber with tensile strength at about 5.694 MPa (Lani et al., 2014). This could be due to the presence of hydrogen bonds between CNC and PVA and the electrostatic interactions between CNC and chitosan, which strengthened the material network and significantly improved the tensile strength of the film. In addition, the uniform dispersion of the system is also vital in increasing the interaction between the CNC and the PVA/CS matrix (Wang et al., 2018). Therefore, the incorporation of PEG, although low in quantity (0.02 %), was necessary to aid the dispersion and enhance the tensile strength of PVA/CS film.
Another crucial criterion in biocomposite films is their swelling properties. When water vapor enters the physical skeleton, it changes the chemical structure of the polymer, resulting in increased free volume and a more open membrane structure. This allows soluble molecules to pass through during gas separation, affects permeability, selectivity, as well as mechanical properties of the membrane (Jahan et al., 2018). From the results obtained from swelling experiments (Figure 5), the addition of CNC to the film decreased the swelling. After 2 h of soaking, PVA/CS film swelled up to 442.13 % and PVA/CS/CNC to 282.14 %. The addition of CNC decreased the swelling by almost 160 % compared to the original PVA/CS film. The presence of strong electrostatic bond between chitosan and CNC, as well as the hydrogen bond between PVA, chitosan, and CNC, strengthens the lattice structure and restricts the flexibility of the PVA molecular chain. This interferes the water permeation pathway and significantly improves the waterproofing properties of PVA/CS films.

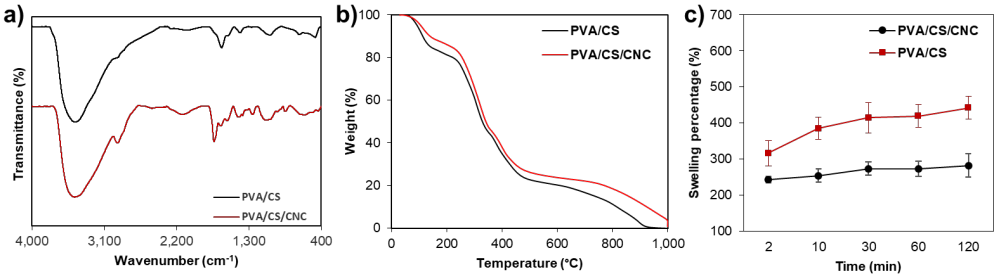

Figure 5: FTIR spectra (a), TGA diagram (b), and swelling properties (c) of PVA/CS and PVA/CS/CNC films.

4. Conclusions

In this study, a simple and chemical-efficient process to produce CNC from PLs was developed. The two-stage alkali treatment followed by bleaching successfully isolated cellulose-rich pulp from PLs with 91.66 % cellulose content. CNC with enhanced dispersibility through the addition of polyethylene glycol (PEG) was then produced using the chemo-mechanical method. The incorporation of CNC improved the mechanical properties of biodegradable PVA/CS film, with a 60 % increase in tensile strength and enhanced waterproofing properties. Based on the findings, the advanced chemo-mechanical method proved its effectiveness in generating high-value engineering CNC from inexpensive PL, presenting a potential material in the structural reinforcement of biocomposite films and aiming towards sustainable development of PL agro-waste.

Acknowledgments

This research is funded by Vietnam National University HoChiMinh City (VNU-HCM) under grant number 562-2022-20-04. We acknowledge the support of time and facilities from Ho Chi Minh City University of Technology (HCMUT), VNU-HCM for this study.

References

Amara C., El Mahdi A., Medimagh R., Khwaldia K., 2021, Nanocellulose-based composites for packaging applications, Current Opinion in Green and Sustainable Chemistry, 31, 100512.
Asim M., Abdan K., Jawaid M., Nasir M., Dashtizadeh Z., Ishak M.R., Hoque M.E., 2015, A Review on Pineapple Leaves Fibre and Its Composites, International Journal of Polymer Science, 2015, 950567.
Balakrishnan P., Sreekala M.S., Kunaver M., Huskić M., Thomas S., 2017, Morphology, transport characteristics and viscoelastic polymer chain confinement in nanocomposites based on thermoplastic potato starch and cellulose nanofibers from pineapple leaf, Carbohydrate Polymers, 169, 176-188.

C.S J.C., George N., Narayanankutty S.K., 2016, Isolation and characterization of cellulose nanofibrils from arecanut husk fibre, Carbohydrate Polymers, 142, 158-166.

Cheng D., Wen Y., Wang L., An X., Zhu X., Ni Y., 2015, Adsorption of polyethylene glycol (PEG) onto cellulose nano-crystals to improve its dispersity, Carbohydrate Polymers, 123, 157-163.

Cherian B.M., Leão A.L., de Souza S.F., Thomas S., Pothan L.A., Kottaisamy M., 2010, Isolation of nanocellulose from pineapple leaf fibres by steam explosion, Carbohydrate Polymers, 81(3), 720-725.

El Achaby M., El Miri N., Aboulkas A., Zahouily M., Bilal E., Barakat A., Solhy A., 2017, Processing and properties of eco-friendly bio-nanocomposite films filled with cellulose nanocrystals from sugarcane bagasse, International Journal of Biological Macromolecules, 96, 340-352.

El Miri N., Abdelouahdi K., Zahouily M., Fihri A., Barakat A., Solhy A., El Achaby M., 2015, Bio-nanocomposite films based on cellulose nanocrystals filled polyvinyl alcohol/chitosan polymer blend, Journal of Applied Polymer Science, 132.

Ibrahim N., Shahar F., Hameed Sultan M.T., Md Shah A., Safri S., Mat Yazik M.H., 2021, Overview of Bioplastic Introduction and Its Applications in Product Packaging, Coatings, 11, 1423.

Ismail M., Ibrahim A., Wan Yaacob W.M.H., mamat razali n.a., Hawa A., Aziz F., 2018, Characteristics of cellulose extracted from Josapine pineapple leaf fibre after alkali treatment followed by extensive bleaching, Cellulose, 25.

Jahan Z., Niazi M.B.K., Gregersen Ø.W., 2018, Mechanical, thermal and swelling properties of cellulose nanocrystals/PVA nanocomposites membranes, Journal of Industrial and Engineering Chemistry, 57, 113-124.

Khalid M.Y., Al Rashid A., Arif Z.U., Ahmed W., Arshad H., 2021, Recent advances in nanocellulose-based different biomaterials: types, properties, and emerging applications, Journal of Materials Research and Technology, 14, 2601-2623.

Lani N., Ngadi N., Johari A., Jusoh M., 2014, Isolation, Characterization, and Application of Nanocellulose from Oil Palm Empty Fruit Bunch Fiber as Nanocomposites, Journal of Nanomaterials, 2014, 1-9.

Mahardika M., Abral H., Kasim A., Arief S., Asrofi M., 2018, Production of Nanocellulose from Pineapple Leaf Fibers via High-Shear Homogenization and Ultrasonication, 6(2), 28.

Mussatto S., Rocha G., Roberto I., 2008, Hydrogen peroxide bleaching of cellulose pulps obtained from brewer's spent grain, Cellulose, 15, 641-649.

Nair S.S., Zhu J.Y., Deng Y., Ragauskas A.J., 2014, High performance green barriers based on nanocellulose, Sustainable Chemical Processes, 2(1), 23.

Nguyen C.T.X., Bui K.H., Truong B.Y., Do N.H.N., Le P.T.K., 2021, Nanocellulose from Pineapple Leaf and Its Applications towards High-value Engineering Materials, Chemical Engineering Transactions, 89, 19-24.

Plermjai K., Boonyarattanakalin K., Mekprasart W., Pavasupree S., Phoohinkong W., Pecharapa W., 2018, Extraction and characterization of nanocellulose from sugarcane bagasse by ball-milling-assisted acid hydrolysis. Vol 2010.

Reshmy R., Philip E., Paul S.A., Madhavan A., Sindhu R., Binod P., Pandey A., Sirohi R., 2020, Nanocellulose-based products for sustainable applications-recent trends and possibilities, Reviews in Environmental Science and Bio/Technology, 19(4), 779-806.

Santos R.M.d., Flauzino Neto W.P., Silvério H.A., Martins D.F., Dantas N.O., Pasquini D., 2013, Cellulose nanocrystals from pineapple leaf, a new approach for the reuse of this agro-waste, Industrial Crops and Products, 50, 707-714.

Selvamurugan M., Pramasivam S., 2019, Bioplastics – An Eco-friendly Alternative to Petrochemical Plastics, Current World Environment, 14, 49-59.

Shahbandeh. M., 2021, Global pineapple production 2002-2019, <statista.com/statistics/298505/global-pineapple-production> accessed.2021.

Shojaeiarani J., Bajwa D.S., Chanda S., 2021, Cellulose nanocrystal based composites: A review, Composites Part C: Open Access, 5, 100164.

Trache D., Tarchoun A.F., Derradji M., Hamidon T.S., Masruchin N., Brosse N., Hussin M.H., 2020, Nanocellulose: From Fundamentals to Advanced Applications, 8(392).

Wang D., Cheng W., Yue Y., Xuan L., Ni X., Han G., 2018, Electrospun Cellulose Nanocrystals/Chitosan/Polyvinyl Alcohol Nanofibrous Films and their Exploration to Metal Ions Adsorption, 10(10), 1046.

Xia Q., Chen C., Yao Y., Li J., He S., Zhou Y., Li T., Pan X., Yao Y., Hu L., 2021, A strong, biodegradable and recyclable lignocellulosic bioplastic, Nature Sustainability, 4(7), 627-635.

Zhang B., Huang C., Zhao H., Wang J., Yin C., Zhang L., Zhao Y., 2019, Effects of Cellulose Nanocrystals and Cellulose Nanofibers on the Structure and Properties of Polyhydroxybutyrate Nanocomposites, Polymers (Basel), 11(12), 2063.